Lyapunov stability analysis of nonlinear dynamics of sound generation in a mixing layer

By Z.-N. Wang†, N. Chandramoorthy‡, P. G. Tucker†, Q. Wang ¶, A. Towne AND S. K. Lele

1. Motivation and objectives

As air traffic volume continues to increase, aircraft noise becomes a greater concern to airport neighbouring residents. Noise is now considered an important certification index for newly developed aircrafts before they enter commercial service. Noise from aircraft is mainly generated aerodynamically, so to understand and reduce it, the research field of aeroacoustics was founded by Sir Micheal James Lighthill in the 1950s (Lighthill 1952a,b). Since then, considerable progress has been made in this field, but fundamental questions about which flow processes are responsible for noise generation have not yet been completely answered (Lele & Nichols 2014). Recently, through both experimental measurements and high-fidelity simulations, large-scale coherent structures have been identified within turbulent jets and mixing layers and been found to be highly correlated to sound generation (Jordan & Colonius 2013). Linear analysis based on the mean flow was developed to successfully replicate these near-field coherent structures (referred to as wave packets) in statistics but this method significantly underpredicts the far-field sound level for subsonic jets (Baqui *et al.* 2013; Jordan *et al.* 2014). This indicates that some fundamental mechanisms in sound generation are still missing. In this context, the nonlinear dynamics are considered as the missing piece of the puzzle in the sound sources but how nonlinear dynamics take place in sound production is still unknown. Hypotheses have been proposed to express nonlinearity in the present frame of linear analysis (Towne *et al.* 2018), but the improvement has not been fully satisfactory yet since not all the missing far-field sound has been compensated (Jordan *et al.* 2014; Towne *et al.* 2015). Therefore, a comprehensive understanding of the full noise production processes, especially the nonlinear process, is crucial to sound source modeling and effective noise reduction.

To characterize nonlinear dynamics, the Russian mathematician Aleksandr M. Lyapunov introduced the exponents of growth rate at the beginning of the 19th century (Lyapunov 1892). Although Lyapunov exponents (LEs) have been theoretically proved to be a coordinate-independent indicator of dynamic regimes, their usefulness had not been fully realized until effective algorithms were proposed (Benettin *et al.* 1967; Shimada & Nagashima 1979). The same story also applies to covariant Lypaunov vectors (CLVs). They were proposed three decades ago (Ruelle 1979) but have been used only in recent years when practical algorithms were developed (Ginelli *et al.* 2007). CLVs are able to offer the intrinsic tangent-space decomposition for any invertible dynamical system and have been successfully used to better understand many aspects of chaotic

† Department of Engineering, University of Cambridge, UK
‡ Department of Mechanical Engineering, Massachusetts Institute of Technology
¶ Department of Aeronautics and Astronautics, Massachusetts Institute of Technology

dynamics. Applications in fluid mechanics field began to be seen recently, such as assessing the dynamic content of the LES (Nastac *et al.* 2017) and investigating the nonlinear mechanisms of turbulence in plane Couette flows (Nikolaidis *et al.* 2018).

Eddy-resolving simulations, including direct numerical simulation (DNS) (Freund 2001), large-eddy simulation (LES) (Shur *et al.* 2003; Bodony & Lele 2008) and hybrid LES-RANS (Tyacke *et al.* 2017; Wang *et al.* 2019), have accurately predicted turbulence and its generated acoustics from first principles. The richness of this time-accurate simulation data provides greater opportunities than ever before to explore the flow processes which contribute to sound generation (Lele & Nichols 2014). With the growth of computational power and the development of numerical algorithms, it is now possible to use hybrid LES-RANS to simulate industry-level, complex-geometry propulsive jets by resolving large-scale turbulent eddies and to evaluate noise reduction strategies at an affordable cost(Wang *et al.* 2019). This enables designers to broaden the traditional design boundaries towards an optimal level where the current design systems fails. Optimization based on this high-fidelity approach could be used to explore the full design space for even quieter jets, which could never be achieved by current approaches.

The research in this report characterizes the nonlinear dynamic process of noise generation in a mixing layer by combining eddy-resolving simulation and Lyapunov analysis. The computed LEs and CLVs can be used in the future for computation of adjoint sensitivity of noise sources and optimization of noise reduction strategies. The report is organized as follows: Section 2 introduces the methodology of computing LEs and CLVs using LES. Section 3 describes the mixing layer case used in this research and clarifies the link to jet noise. The nonlinear dynamics of sound generation revealed by the computed LEs and CLVs is outlined in Section 4. Finally, key conclusions are drawn and future work is outlined in Section 5.

2. Methodology: LES and Lyapunov stability analaysis

The mixing layer is time-accurately resolved using large-eddy simulation (LES), which is combined with Lyapunov analysis to obtain the nonlinear dynamical response of a mixing layer.

2.1. *Large-eddy simulation*

In LES, an unstructured, edge-based finite-volume compressible flow solver is used to simulate mixing layer flows and a portion of near-field acoustics. LES requires numerical schemes of low dissipation; hence, a non-dissipative kinetic energy preserving (KEP) scheme (Jameson 2008), which substantially improves turbulence resolution compared to the upwinding, Roe scheme, has been implemented. This KEP scheme is computationally stable without numerical dissipation and shows low sensitivity to the grid types, which assures the quality of LES solutions on unstructured meshes (Tyacke *et al.* 2017). The flow field is advanced in time using the five-stage explicit Runge-Kutta method. The wall-adapting local eddy-viscosity (WALE) model (Nicoud & Ducros 1999) is used to model unresolved turbulence scales in the LES computation. The sponge region and characteristic boundary conditions are employed to reduce reflections from computational boundaries. The code shows almost linear scaling over 10000 cores using MPI with parallel I/O implemented by HDF5 libraries. This flow solver is well validated and used to predict flows and acoustics of propulsive jet flows from canonical to industrial levels (Wang *et al.* 2019).

2.2. *Lyapunov stability analysis*

Upon spatial discretization, the flow governing equations can be written in the form of

$$\frac{du}{dt} = f(u),\ u(t_0) = u_0(\phi), \tag{2.1}$$

where $u(t)$ is a n-dimensional vector of conservative flow variables, i.e., density, momentum and total energy, on every grid point at the time instant t. $f(u)$ is the steady Navier-Stokes equation operator, including convective, viscous flux and source terms if applicable. ϕ is a parameter which characterizes the initial flow condition.

The homogeneous tangent vector $w = du/d\phi$ characterizes the flow response to initial perturbations. The tangent equation can be obtained from Eq. (2.1) and is written as

$$\frac{dw}{dt} = \left.\frac{df}{du}\right|_{u(t)} w, \tag{2.2}$$

where df/du is a $n \times n$ matrix and $w(t)$ is the tangent vector, which is of the same dimension as $u(t)$.

Suppose the chaotic system (Eq. (2.1)) is ergodic and that there exists n LEs $\lambda^1 \geq \lambda^2 \geq \cdots \geq \lambda^n \in \mathbf{R}$ and n corresponding CLVs $\psi^1(u), \psi^2(u), \cdots, \psi^n(u) \in \mathbf{R}^n$. The CLVs form a basis for the solution to Eq. (2.2). That is, a tangent solution $w(t)$ can be written as a linear combination of the CLVs. Any infinitesimal perturbation $\delta u(t_0)$ in the direction of CLV $\psi^j(u(0))$ will stay in the $\psi^j(u(t))$ for $t \geq t_0$, and the magnitude of this perturbation decreases or increases at an asymptotic rate in time, i.e., $\|\delta u(t)\| \sim \|\delta u(t_0)\| e^{\lambda^j (t-t_0)}$. Hence, the LEs λ^j and their corresponding CLVs $\psi^j(u)$ characterize the dynamic system (Eq. (2.1)). Depending on the sign of the LEs, the tangent modes $\psi^j(u)$ of the nonlinear system (Eq. (2.1)) can be divided into three regimes: unstable for $\lambda^j > 0$, neutral for $\lambda^j = 0$ and stable for $\lambda^j < 0$.

The procedure for calculating LEs and CLVs follows the dynamic algorithm (Ginelli *et al.* 2007) with the homogeneous tangent equation Eq. (2.2) solved using numerical differentiation between the perturbed and base flow trajectories.

(*a*) Forward process: Given an initial vector u_0 in phase space and an initial set of randomly perturbed orthogonal vectors $\{q_0^j\}_{j=1,\cdots,n}$ in tangent space, evolve the phase and tangent dynamics by solving Eq. (2.1) and Eq. (2.2) over time segments. At the end of each time segment i, perform QR decomposition on the tangent matrix $W_i = [w_i^1, w_i^2, \cdots, w_i^n]$ to obtain $W_i = Q_i R_i$, where $Q_i = [q_i^1, q_i^2, \cdots, q_i^n]$. Take u_i and $\{q_i^j\}_{j=1,\cdots,n}$ as the initial condition for the next segment $i+1$ evolution. Repeat the process for $m+l$ segments, where both the phase space and the tangent space converge at the segment m. The LEs can be obtained by averaging the diagonal components of R_i

$$\lambda^j = \frac{1}{l} \sum_{i=m+1}^{m+l} \log(|R_i^{j,j}|), \tag{2.3}$$

(*b*) Backward process: The CLVs can be expressed as a combination of an orthogonal basis by using $\{c_i^{k,j}\}$ starting from $i = l$. Then,

$$\psi_i^j = \sum_{k=1}^{j} c_i^{k,j} q_i^k \tag{2.4}$$

The expansion coefficients $c_i^{k,j}$ form an upper-triangular matrix $C_i = \{c_i^{k,j}\}_{k \leq j = 1,2,\cdots,n}$.

Given a generic nonsingular upper-triangular matrix C_{m+l}, evolve it backward in time along the obtained flow trajectory by $C_i = R_{i+1}^{-1} C_{i+1}$ and then $Q_i C_i$ will converge to the true CLVs ψ_i^j over p time segments. To prevent exponential growth of C_i, every element $c_i^{k,j}$ is normalized by its diagonals $c_i^{j,j}$ for each time segment. Continue this backward process until the time segment m; the CLVs ψ_i^j can be obtained for the segment $i = m, m+1, \cdots, m+l-p$.

3. Simulation setup

The case investigated in this paper is mixing layer noise. The mixing layer shares many ingredients with jet flows before the end of potential in noise generation. Direct numerical simulation (DNS) of mixing layers has been used to study the sound generation process and evaluate acoustic analogy by Colonius *et al.* (1997). The mixing layer used in the current research is formed by two streams of fluid passing a plate splitter. The stream at the lower side is at $Ma_{low} = 0.5$, while the stream at the upper side is at $Ma_{up} = 0.25$. The Reynolds number $Re_{\delta^*} = \rho U_{low} \delta^* / \mu$ is 300, which is based on the lower-side stream velocity U_{low} and the displacement thickness δ^* at the plate trailing edge. It was simulated using LES and analyzed using LEs and CLVs. The computational domain size is $2000\delta^* \times 50\delta^* \times 1000\delta^*$ in the x (streamwise), y (spanwise) and z (transverse) directions, where the LES region is focused within $550\delta^* \times 50\delta^* \times 600\delta^*$ surrounded by sponge regions. The Kelvin-Helmholtz instability develops at around $x/\delta^* = 100$ and vortices begin to form and pair up from $x/\delta^* = 200$. The spanwise vorticity and streamwise vorticity at the $y = 0$ plane are shown in Fig. 1. The time step in LES is $0.02\delta^*/U_{low}$ and the time segment length in the Lyapunov analysis contains 10,000 time steps, which is approximately equal to one period of vortex pairing.

4. Results and discussions

Lyapunov stability analysis is obtained by perturbing the flow around a spatio-temporal evolving trajectory of chaotic flows $u(t)$, which is different from that of convectional linear stability analysis around a mean flow base. For every initial perturbation, there is a corresponding path that the perturbed flow follows. The growth/decay rate of the perturbation along this path is defined by the LE. The Lyapunov spectrum consists of all the LEs, which characterize the dynamical system. The CLV represents the path/direction in which the perturbation will develop under the control of the associated LE. In this section, the Lyapunov spectrum, with the corresponding CLVs on mixing layer flows and their corresponding near-field acoustics, has been obtained. Each LE and CLV constitutes one dynamical mode that characterizes the nonlinear response of mixing layer flows. Hence, sound generation in these dynamical modes is discussed, which could provide an unique insight from a nonlinear dynamics perspective.

4.1. *Lyapunov spectrum*

To obtain the Lyapunov spectrum, the first 150 largest LEs for this mixing layer flow have been computed. Figure 2(a) shows that the convergent LEs are obtained after 40 time segments, and 98 time segments have been calculated. The computed Lyapunov spectrum is shown in Figure 2(b). Among these 150 LEs, there are about 100 unstable modes and 50 stable modes and the neutral mode sits around the 100th. The 1st/leading positive LE determines the largest growth rate of the nonlinear system instability. Moving to higher

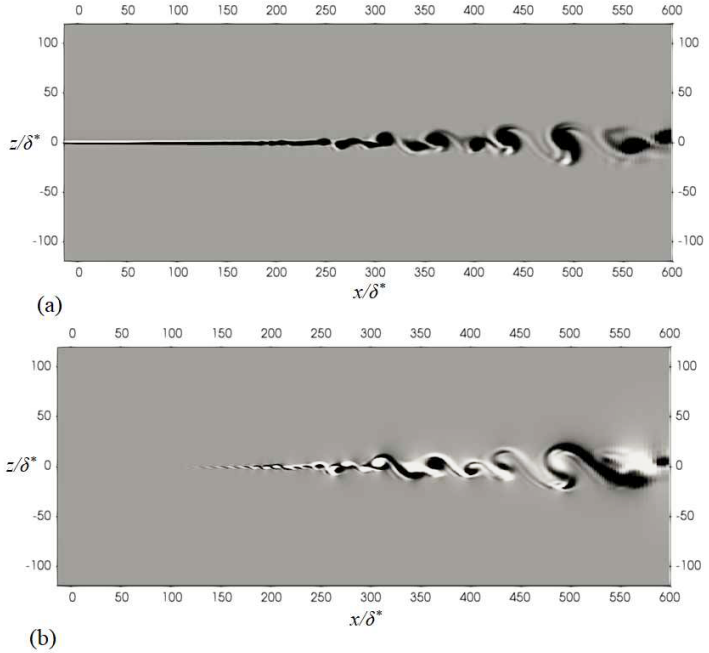

FIGURE 1. Snapshots of (a) spanwise vorticity and (b) streamwise vorticity in mixing layer flows at the $y = 0$ plane.

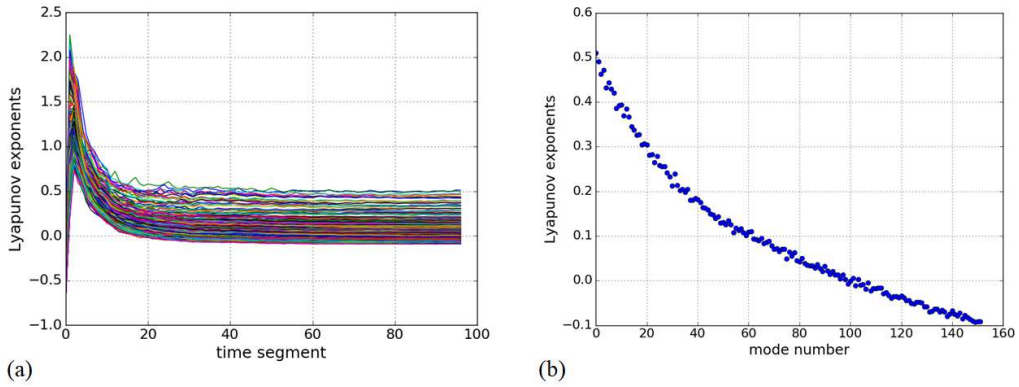

FIGURE 2. (a) Convergence history and (b) convergent spectrum of the first 150 Lyapunov exponents (LEs).

modes with smaller positive LEs, the growth rates decrease, where the perturbed flow diverges more slowly from the original trajectory than that of the previous LEs. When LEs approach zero, the neutral mode is reached, where the magnitude of perturbations is maintained. For negative LEs, the perturbation decays and the perturbed flow finally returns to its baseline trajectory. Hence, only the 100 unstable modes with positive LEs contribute to the dynamical system response to initial perturbations in this mixing layer case.

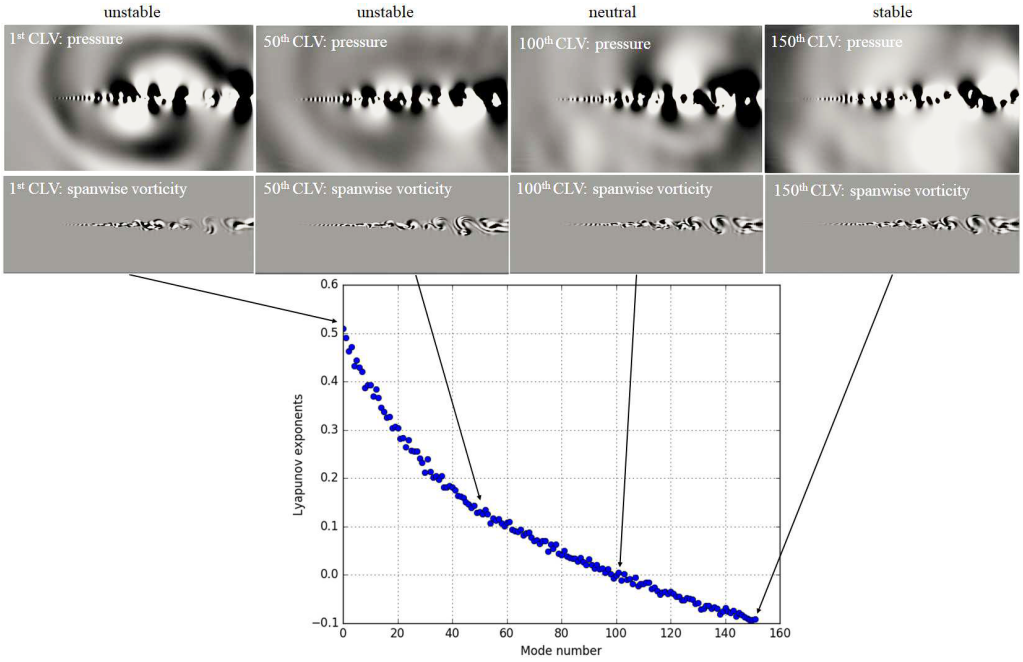

FIGURE 3. Pressure and spanwise vorticity components of covariant Lyapunov vectors (CLVs) with their corresponding exponents.

4.2. *Covariant Lyapunov vectors*

CLVs identify the expanding and contracting directions of a given dynamical system. They provide the routes $\psi^j(u(t))$, whose stability properties are ruled by the associated LEs λ^j, for the initial perturbations' evolution based on the given flow trajectory $u(t)$. Figure 3 shows snapshots of the CLVs computed at the same instant using the dynamic algorithm given in Section 2. Four typical dynamic modes are selected: the leading unstable mode (1st CLV), the intermediate unstable mode (50th CLV), the neutral mode (100th CLV) and the stable mode (150th CLV). The pressure and spanwise vorticity components of these four CLVs are shown with the same contour levels for comparison. The 1st CLV is associated with the largest growth rate, which is the most unstable mode. The CLV pressure component shows obvious sound generation in this leading mode. As it is moved toward a higher number of unstable modes, the sound generation gets weaker. For neutral and stable modes, the sound generation from the shear layer is less obvious. The vorticity in the leading modes is more concentrated at the upstream of the shear layer, while it is distributed more towards downstream as moved towards neutral and stable modes because large-scale mixing takes place downstream to dissipate the kinetic energy.

Since the CLVs $\psi^j(u(t))$ depend on the local phase state $u(t)$, hence their development around the base flow trajectory $u(t)$ can be used to show the nonlinear dynamics of sound generation events inside the mixing layer. Figure 4 shows the time series of the 1st and 50th CLV pressure and spanwise vorticity along with the base flow spanwise vorticity. Acoustic waves emitted from mixing layers are visible in the CLV pressure components. Two sound generation events are locked through three frameworks using the dashed lines to identify the possible cause. The base flow vorticity and CLV vorticity show that sound

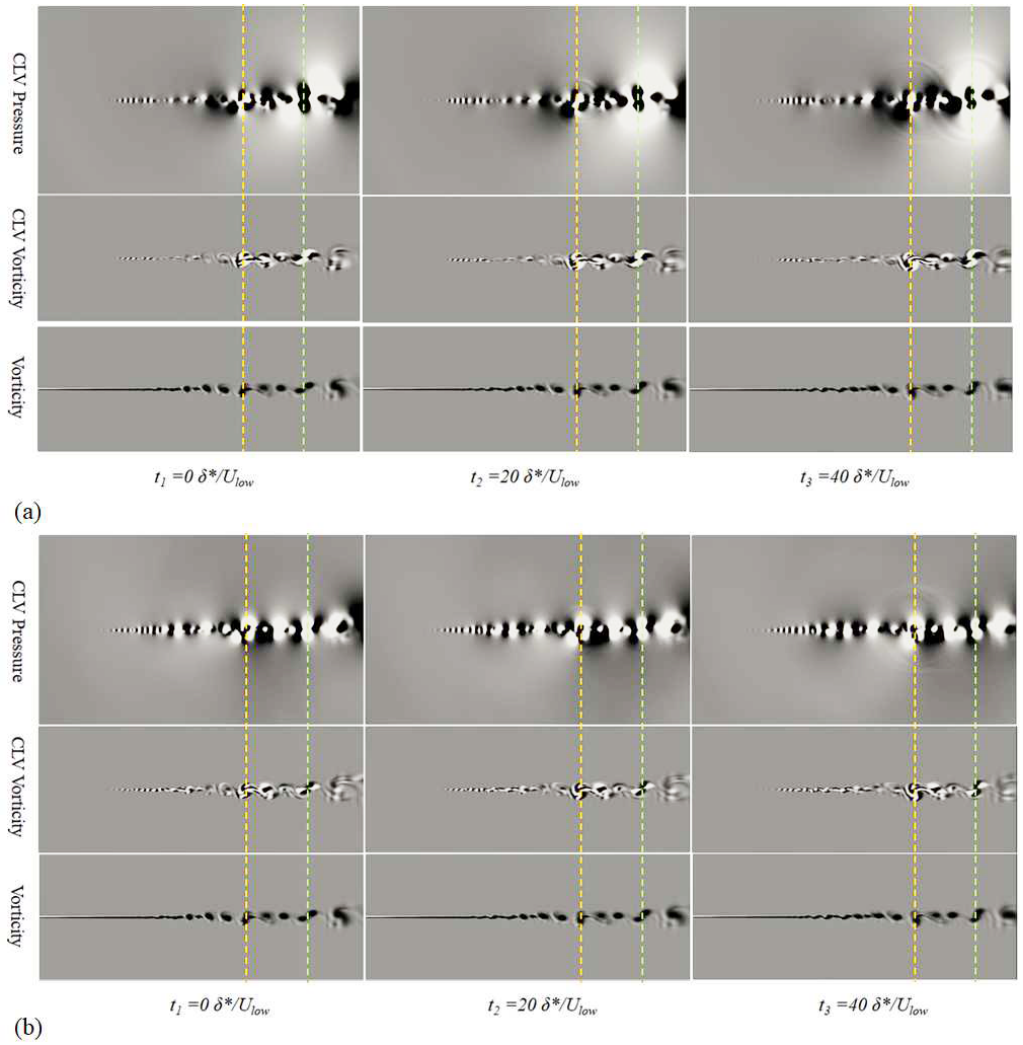

FIGURE 4. Sound generation events in the (a) 1st and (b) 50th CLVs

generation is highly correlated with the vortex shedding and pairing inside the mixing layer. The sound generation gets weaker and less visible in the 50th CLV than in the leading CLV, especially for the downstream sound generation event. This indicates that the instability growth rate could determine the sound generation strength.

4.3. *Spectral analysis of the unstable CLVs*

As shown in Figure 4, acoustic waves are produced in the unstable CLVs, spectral analysis of the radiated acoustics is performed in each dynamical mode to further understand the frequency response. An array of probes are placed at the tranverse distance of $z = 150\delta^*$. This is sufficiently far from the hydrodynamic region of the mixing layer. The probe locations are converted to observation polar angles, with the origin located at the vortex-shedding location $(x/\delta^*, z/\delta^*) = (200, 0)$.

Figure 5 shows the pressure spectra of two typical unstable CLVs (the 1st and 50th)

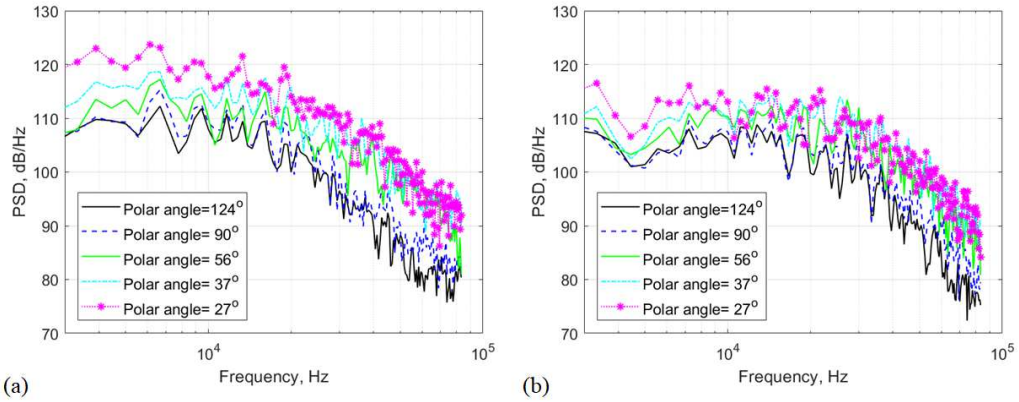

FIGURE 5. Pressure spectra of the (a) 1st and (b) 50th unstable covariant Lyapunov vectors (CLVs) at five observed locations.

at five probe locations. The acoustic energy increases when the observer is moving to downstream positions. This is consistent with the super-directivity of shear-layer acoustic sources (Crighton & Huerre 1990). Differences between the two CLVs' pressure spectra are also seen. The 1st CLV shows more rapid decay at high frequencies while the 50th CLV exhibits a broadening of spectra for all the angles. For any fixed angle, the 50th CLV contains less energy at low frequencies than the 1st CLV does. This indicates that lower modes of CLVs with larger positive LEs might contribute more to low-frequency acoustic production.

5. Summary and future work

Lyapunov stability analysis combined with LES has been performed on a mixing layer at $Re_{\delta^*} = 300$. The first 150 LEs along with the corresponding CLVs are obtained and the neutral mode is reached at approximately the 100th LE. CLVs characterize the dynamical response to the nonlinear system of a mixing layer and are used to analyze the sound generation inside the shear layer. Sound generation and acoustic radiation are visible in the unstable CLVs but get weaker for the CLVs of smaller positive LEs. The sound generation events in the CLVs can be linked with vortex shedding and pairing in the shear layer. Spectral analysis of the unstable CLV pressure shows that acoustic super-directivity also exists in the dynamical modes and that the acoustic spectra tend to broaden at all the observation angles with a decrease of low-frequency energy for the CLVs with smaller LEs. This implies that the CLVs associated with larger LEs could contribute more to low-frequency noise in this mixing layer flow.

Future research is expected to take two directions: First, the CLVs will be compared with linear stability analysis to explore the role of nonlinear dynamics in sound generation; Second, the LEs and CLVs will be used to compute sensitivity information and optimize the plate trailing edge shape for noise reduction using the least-squares shadowing methods (Ni & Wang 2017; Blonigan 2017) or the newly developed space-split method (Chandramoorthy *et al.* 2018).

Acknowledgments

The authors very much appreciate the fruitful discussions with and advice from other summer program participants, especially Drs. Sanjeeb Bose, Patrick Blonigan and Oliver

Schmidt; Profs. Peter Schmid and Gianluca Iaccarino; and the kind host from Prof. Parviz Moin. The computations were performed on the UK national supercomputing facility ARCHER via UK Turbulence Consortium (EP/R029326/1).

REFERENCES

Baqui, Y. B., Agarwal, A., Cavalieri, A. V. G. & Sinayoko, S. 2013 Nonlinear and linear noise source mechanisms in subsonic jets. *AIAA Paper* 2013-2087.

Benettin, G., Galgani, L., Giorgilli, A. & Strelcyn, J. M. 1967 Lyapunov characteristic exponents for smooth dynamical systems and for Hamiltonian systems; a method for computing all of them. Part 1: Theory. *Meccanica* **15**, 9–20.

Blonigan, P. J. 2017 Adjoint sensitivity analysis of chaotic dynamical systems with non-intrusive least squares shadowing. *J. Comput. Phys.* **348**, 803–826.

Bdony, D. J. & Lele, S. K. 2008 Current status of jet noise predictions using Large-Eddy Simulation.*J. Comput. Phys.* **348**, 803–826.

Chandramoorthy, N., Wang, Z.-N., Wang, Q. & Tucker, P. G. 2018 Towards computing sensitivities of average quantities in turbulent flows. *Proceedings of the Summer Program*, Center for Turbulence Research, Stanford University.

Colonius, T., Lele, S. K. & Moin, P. 1997 Sound generation in a mixing layer. *J. Fluid Mech.* **330**, 375–409.

Crighton, D. G. & Huerre, P. 1990 Shear-layer pressure fluctuations and superdirective acoustic sources. *J. Fluid Mech.* **220**, 355–368.

Freund, J. B. 2001 Noise sources in a low-Reynolds-number turbulent jet at Mach 0.9. *J. Fluid Mech.* **438**, 227–305.

Ginellin, F., Poggi, A., Turchi, A., Chate, H., Livi, R. & Politi, A. 2007 Characterizing dynamics with covariant lyapunov vectors. *Phys. Rev. Lett* **99**, 130601.

Jameson, A. 2008 Formulation of kinetic energy preserving conservative schemes for gas dynamics and direct numerical simulation of one-dimensional viscous compressible flow in a shock tube using entropy and kinetic energy preserving schemes. *J. Sci. Comput.* **34**, 188–208.

Jordan, P. & Colonius, T. 2013 Wave packets and turbulent jet noise. *Annu. Rev. Fluid Mech.* **45**, 173–195.

Jordan, P., Colonius, T., Bres, G. A., Zhang, M., Towne, A., & Lele, S. K. 2014 Modeling intermittent wavepackets and their radiated sound in a turbulent jet. *Proceedings of the Summer Program*, Center for Turbulence Research, Stanford University, pp. 241–248.

Lele, S. K. & Nichols, J. W. 2014 A second golden age of aeroacoustics? *Philos. Trans. Royal Soc. A* **372**, 20130321.

Lighthill, M. J. 1952 On sound generated aerodynamically. I. General theory. *Proc. Royal Soc. Lond. A* **211**, 564–587.

Lighthill, M. J. 1952 On sound generated aerodynamically. II. Turbulence as a source of sound. *Proc. Royal Soc. Lond. A* **222**, 1–32.

Lyapunov, A. M. 1892 *The general problem of the stability of motion* (in Russian). Ph.D. Thesis, University of Kharkov.

Nastac, G., Labahn, J. W., Magri, L. & Ihme, M. 2017 Lyapunov exponent as a metric for assessing the dynamic content and predictability of large-eddy simulations. *Phys. Rev. Fluids* **2**, 094606.

Ni, A. & Wang, Q. 2017 Sensitivity analysis on chaotic dynamical systems by non-intrusive least squares shadowing (NILSS). *J. Comput. Phys.* **347**, 56–77.

Nicoud, F. & Ducros, F. 2017 Subgrid-scale stress modelling based on the square of the velocity gradient tensor. *Flow, Turbul. Combust.* **62**, 183–200.

Nikolaidis, M.-A., Farrell, B. F. & Ioannou, P. J. 2018 The mechanism by which nonlinearity sustains turbulence in plane Couette flow. *J. Phys. Conf. Ser.* **1001**, 012014.

Ruelle, D. 2018 Ergodic theory of differentiable dynamical systems. *Publ. Math. IHES* **50**, 27–58.

Shimada, I. & Nagashima, T. 1979 A Numerical Approach to Ergodic Problem of Dissipative Dynamical Systems. *Prog. Theor. Phys.* **61**, 1605.

Shur, M. L., Spalart, P. R., Strelets, M. K. & Travin, A. K. 2003 Towards the prediction of noise from jet engines. *Int. J. Heat Fluid Fl.* **24**, 551–561.

Towne, A., Colonius, T., Jordan, P., Cavalieri, A. V., & Bres, G. A. 2015 Stochastic and nonlinear forcing of wavepackets in a Mach 0.9 jet. *AIAA Paper* 2015-2217.

Towne, A., Schmidt, O. T., & Colonius, T. 2018 Spectral proper orthogonal decomposition and its relationship to dynamic mode decomposition and resolvent analysis. *J. Fluid Mech.* **847**, 827–867.

Tyacke, J. C., Naqavi, I. Z., Wang, Z.-N., Tucker, P. G. & Boehning, P. 2017 Predictive LES for jet aeroacoustics - current approach and industrial application. *J. Turbomach.* **139**, 081003.

Wang, Z.-N., Tyacke, J. C., Tucker, P. G. & Boehning, P. 2019 Parallel computation of aeroacoustics of industrially relevant complex-geometry aeroengine jets. *Comput. Fluids* **178**, 166-178.